

Metrics for Developing an Endorsed Set of Radiographic Threat Surrogates for JINII/CAARS

Ron Wurtz, Sean Walston, Dan Dietrich, Harry Martz
Lawrence Livermore National Laboratory
Livermore, CA 94551

Work performed on the
Science & Technology Directorate of the
Department of Homeland Security
Statement of Work

IAA No. HSHQDC-08-X-00388

18 February 2009
LLNL-SR-411173



 **Lawrence Livermore
National Laboratory**



This document was prepared as an account of work sponsored by an agency of the United States government. Neither the United States government nor Lawrence Livermore National Security, LLC, nor any of their employees makes any warranty, expressed or implied, or assumes any legal liability or responsibility for the accuracy, completeness, or usefulness of any information, apparatus, product, or process disclosed, or represents that its use would not infringe privately owned rights. Reference herein to any specific commercial product, process, or service by trade name, trademark, manufacturer, or otherwise does not necessarily constitute or imply its endorsement, recommendation, or favoring by the United States government or Lawrence Livermore National Security, LLC. The views and opinions of authors expressed herein do not necessarily state or reflect those of the United States government or Lawrence Livermore National Security, LLC, and shall not be used for advertising or product endorsement purposes.

This work performed under the auspices of the U.S. Department of Energy by Lawrence Livermore National Laboratory under Contract DE-AC52-07NA27344.

Metrics for Developing an Endorsed Set of Radiographic Threat Surrogates for JINII/CAARS

Ron Wurtz, Sean Walston, Dan Dietrich, Harry Martz
Lawrence Livermore National Laboratory
Livermore, CA 94551

Executive Summary

Goal: Develop metrics for dual-energy radiography.

Application: Evaluate surrogate assemblies whose appearance using dual-energy x-ray radiography systems is indistinguishable from real threat assemblies that the systems are required to alarm on.

Metrics developed: We have defined two metrics. They are derived from the photon flux density transmitted along an idealized bremsstrahlung ray through an assembly.

If the “transmission” is defined as the ratio of transmitted to incident photon flux density, the first metric is the ratio of transmission of a bremsstrahlung ray of one endpoint energy to the transmission of a ray of a higher endpoint energy. The second metric is the number of mean free paths of one of the radiologic non-intrusive inspection beams along the ray, computed by the natural log of the inverse of the transmission.

The first metric tends to increase with increasing Z . The second metric tends to increase with increasing areal density (the product of mass density and thickness) along the ray.

These two metrics are plotted in a Cartesian space as $\left(\frac{I/I_0|_6}{I/I_0|_9}, \ln(I_0/I|_6) \right)$ where 6 and 9 refer to 6 and 9 MeV endpoint bremsstrahlung beams. These metrics are broad enough to cover systems of different source spectra and detector spectral response; in other words, these metrics capture physical properties of the assemblies and not the x-ray radiography systems.

Introduction

CAARS (Cargo Advanced Automated Radiography System) is developing x-ray dual energy and x-ray backscatter methods to automatically detect materials that are greater than $Z=72$ (hafnium). This works well for simple geometry materials, where most of the radiographic path is through one material. However, this is usually not the case. Instead, the radiographic path includes many materials of different lengths. Single energy can be used to compute $\mu\gamma$ (see below) which is related to areal density (mass per unit area) while dual energy yields more information.

Approach

This report describes a set of metrics suitable and sufficient for characterizing the appearance of assemblies as detected by x-ray radiographic imaging systems, such as those being tested by Joint Integrated Non-Intrusive Inspection (JINII) or developed under CAARS. These metrics will be simulated both for threat assemblies and surrogate threat assemblies (such as are found in Roney *et al.* 2007) using geometrical and compositional information of the assemblies. The imaging systems are intended to distinguish assemblies containing high- Z material from those containing low- Z material, regardless of thickness, density, or compounds and mixtures. The systems in question operate on the principle of comparing images obtained by using two different x-ray end-point energies – so-called “dual energy” imaging systems. At the direction of the DHS JINII sponsor, this report does not cover metrics that implement scattering, in the form of either forward-scattered radiation or high- Z detection systems operating on the principle of backscatter detection. Such methods and effects will be covered in a later report. The metrics described here are to be used to compare assemblies and not x-ray radiography systems. We intend to use these metrics to determine whether two assemblies do or do not look the same. We are tasked to develop a set of assemblies whose appearance using this class of detection systems is indistinguishable from the real threats. To check such an indistinguishability, we must define metrics that are broad enough to cover systems of different source spectra and detector spectral response; in other words, the best metrics should capture physical properties of the assemblies and not the source and detectors employed. In fact, one requirement for the metrics is that, as the detection circumstances change, the similarity or difference of the metrics of two assemblies should be maintained.

This report describes the set of two simple “dual energy” metrics that we have selected. A second report (Wurtz, et al. 2009) goes on to demonstrate several characteristics of the metrics, including how sensitive they are (or are not) to changes in the detection systems, shielding, etc.

Attenuation metrics

A radiographic image is a projection in the form of a two-dimensional array of pixels. Each pixel in the image represents the transmission of a penetrating beam of photons projected from a source, through an intervening material or assembly of materials, into a medium sensitive to the photons. Under the completely idealized conditions called “narrow beam geometry” or “good geometry”, a beam of penetrating radiation of photon flux density I moving through an assembly of materials is removed by each layer of intervening material by the differential relation of attenuation

$$dI = -\rho \left(\frac{\mu}{\rho} \right) I dy_l$$

where ρ is the mass density of the material, (μ/ρ) is the mass attenuation coefficient, and y_l is the thickness through one of the intervening materials. This results in the equation for each layer of

$$I = I_0 e^{-\mu y_l}$$

where I_0 is the incident beam, I is the transmitted beam, and μ is the x-ray linear attenuation coefficient (the inverse of the beam's energy-dependent and Z-dependent mean free path through those materials). As the beam travels through the whole assembly, the attenuation is multiplicative, making the exponents additive, and we obtain

$$I = I_0 e^{-\sum_{\text{layer}_i} \mu_i y_{l_i}}$$

The preceding expression can be used when the beam is composed photons of a single energy. In the case of a beam composed of a range of energies, like a bremsstrahlung beam, the complete expressions for the transmitted and incident photon flux density are

$$I = \int_E I_0(E) e^{-\sum_{\text{layer}_i} \mu_i(E) y_{l_i}} dE \quad \text{and} \quad I_0 = \int_E I_0(E) dE$$

For the rest of the discussion, we will refer to I and I_0 as in the above expressions. These are the measured quantities (ignoring real-world corrections made for sources and detectors which we will not deal with in this report) so we move the unknowns to the right side,

$$\frac{I}{I_0} = \frac{\int_E I_0(E) e^{-\sum_{\text{layer}_i} \mu_i(E) y_{l_i}} dE}{\int_E I_0(E) dE}$$

Note that in the ideal case with a single layer and a monoenergetic beam, this can be expressed very naturally using the logarithm as

$$\ln \left(\frac{I_0}{I} \right) = \mu y_l$$

which is simply the number of mean free paths of the beam through the medium. In fact, this causes the log of I/I_0 to be a natural unit regardless of the energy distribution or number of layers.

As an aside, because of this natural unit, one might be tempted to define an effective mu “ μ_{eff} ” by the measured radiographic transmission I/I_0 along a path from source to detector element of known length $y_{l,\text{known}}$,

$$\mu_{\text{eff}} = \frac{1}{y_{l,\text{known}}} \ln \left(\frac{I_0}{I} \right)$$

In a radiographic image, μ_{eff} represents a parameter capable of helping determine the location of high-Z material, where larger μ_{eff} is generally associated with higher-Z material. In reality, even if y_l has been measured, the computed μ_{eff} does not strongly correlate with the presence of high-Z in the intervening material unless it is the dominant material along the line of sight. Similarly, one might be tempted to assume a value of μ

for a known substance (say μ_A) and use I/I_0 to obtain an equivalent path length for that substance

$$l_{A,equiv} = \frac{1}{\mu_A} \ln\left(\frac{I_0}{I}\right).$$

In either case, the only measured quantities are I and I_0 . This report intends to remove itself as much as possible from either knowing y_l or assuming a substance's μ . Stated plainly, our metrics will be based only on I/I_0 (without scattering), effectively the number of mean free paths for the source-assembly-detector setup. If it is true that μ_{eff} or l_{equiv} correlate with Z , then this simple function of I/I_0 will too.

Implementation

A “dual energy” system uses a second source of different energy spectrum to obtain a second radiographic projection image. One records the pair $(I/I_{0|1}, I/I_{0|2})$ for every pixel, where the “1” and “2” signify conditions of the two interrogating beams. The advantage is that, with measurements of transmission at two different energies in each pixel of the image, better Z -dependent distinctions for each pixel can be drawn. Z sensitivity is strongest where μ changes most rapidly with Z and energy. For these simulations of integrated I/I_0 , we follow the convention to choose the two different sources to have 6 and 9 MeV endpoint bremsstrahlung spectra. These two endpoints have been selected by others because they provide differing distributions of photons below and above the boundary in energy where pair production cross-section rises above the Compton scattering cross-section. Regardless of endpoint, both beams are mostly composed of photons below 1.5 MeV. When comparing integrated I/I_0 for 6 and 9 MeV, the cross-section dependence on the Compton to pair production boundary is strongly diluted by integrating in these low-energy photons. To reduce the dilution, we compute integrated I/I_0 cut-on sharply above 1.5 MeV.

Finally, even after making careful spectral selections, although there is a broad range of $(I/I_{0|1}, I/I_{0|2})$ among all the pixels, when these metrics are plotted, all the pixels in an image closely hug the $x=y$ line for almost all values of Z . In order to improve the ability to visually separate distributions of pixels in a dual energy image, we have decided to compute the metrics as

$$\left(\frac{I/I_{0|1}}{I/I_{0|2}}, \ln(I_0/I_{0|1}) \right)$$

so that the x-axis is the slope of the line $(I/I_{0|1}, I/I_{0|2})$ and the y-axis is the number of mean free paths of one of the beams along the ray into the pixel.

To re-iterate: we will compute the attenuation of rays through assemblies into images made of pixels. The two modeled sources will be 6 and 9 MeV endpoint bremsstrahlung, with a low-energy cut-on at 1.5 MeV. We will derive two metrics from these two attenuation images.

For illustration, we have computed these two metrics for ordered pairs (Z, l) of pure elements at the densities they are found at standard temperature and pressure (STP). Z runs from 1 through 99 and y_l runs from 0 to 20 cm. Each element is displayed as a line starting at $(1,0)$, where the thickness is 0 cm and the transmission of each beam is 1.

Because the mean free path through a gas is long compared with 20 cm, gases are scallops at nearly (1,0) in this graph. Al, Fe, Ag, Pb, W, U, and Pu appear in red to guide the eye.

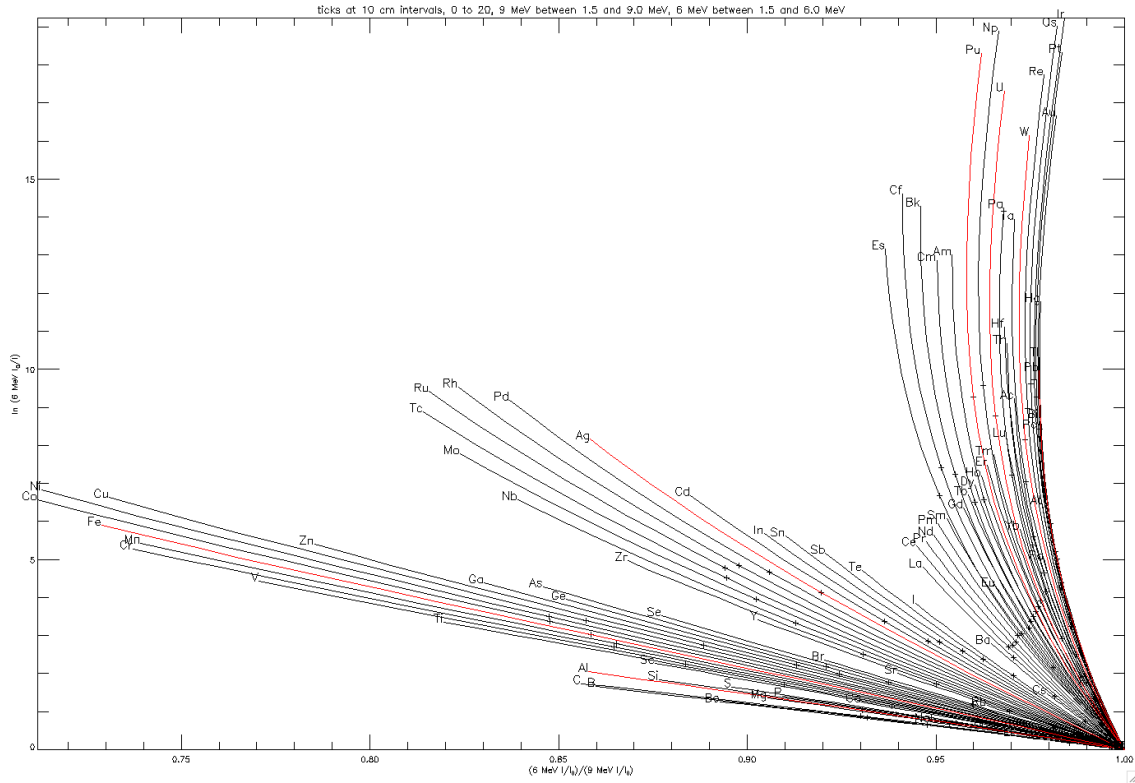


Figure 1: Two radiographic metrics for all elements at STP. See text for explanation.

These metrics will be computed using the HADES code developed at LLNL for radiographic imaging simulations (Aufderheide, *et al.* 2000, 2004). The code will be presented with each assembly to be interrogated and characterized, two planar collimated bremsstrahlung sources of 6 and 9 MeV endpoint with spectra that do not exhibit spatial variations, and a planar detector with a simple boxcar spectral response cut-on at 1.5 MeV and fine spatial sampling. The code will create two images, essentially arrays of pairs of $(I/I_0)_1, (I/I_0)_2$ that can be compared against pixels in images of other assemblies. Because the point is to obtain an ensemble of pixels that can be used to compare two assemblies, these simulations are best described as “idealized”.

References

M. B. Aufderheide, D. M. Slone, A. E. Schach von Wittenau, "HADES, A Radiographic Simulation Code", in *Review of Progress in Quantitative Nondestructive Evaluation*, **20A**, 2000, D. Thompson and D. Chimenti, eds., AIP Conf. Proc. 557, pp. 507-513.

M.B. Aufderheide, G. Henderson, A.E. Schach von Wittenau, D.M. Slone, H.E. Martz, “HADES, a code for simulating a variety of radiographic techniques”, in *2004 IEEE Nuclear Science Symposium Conference Record*, Volume 4, pp. 2579 - 2583, Digital Object Identifier 10.1109/NSSMIC.2004.1462780

“Workshop Summary on Defining SNM and RDD Benchmarks and Cargo Scenes for System Performance of X-ray Radiography Non-Intrusive Inspection Systems,” A Joint Report Produced By: Timothy Roney, Timothy White, Idaho National Laboratory (INL/EXT-07-12199), Maurice B. Aufderheide, Harry E. Martz, Jr., Alan Ross, Dennis R. Slaughter, Padmini R. Sökkappa, Daniel J. Schneberk, Richard M. Wheeler, Lawrence Livermore National Laboratory (UCRL-TR-229119-**REV1**), Ofelia P. Bredt, Robert C. Runkle, John E. Schweppe, Harold E. Trease, Lynn L. Trease, Pacific Northwest National Laboratory (PNNL-16467), Kenneth J. Adams, Eric Tollar, Science Applications International Corporation, May 2007.

Wurtz, R, in preparation.